

Review of modern numerical methods for a simple vanilla option pricing problem

Jiří HOZMAN^{a*}, Dana ČERNÁ^a, Michal HOLČAPEK^b, Tomáš TICHÝ^c, Radek VALÁŠEK^b

^a Department of Mathematics and Didactics of Mathematics, Faculty of Science, Humanities and Education, Technical University of Liberec, Studentská 2, 461 17 Liberec, Czech Republic.

^b Institute for Research and Applications of Fuzzy Modeling, University of Ostrava, 30. dubna 22, 701 03 Ostrava, Czech Republic.

^c Department of Finance, Faculty of Economics, VŠB-Technical University of Ostrava, Sokolská třída 33, 702 00 Ostrava, Czech Republic.

Abstract

Option pricing is a very attractive issue of financial engineering and optimization. The problem of determining the fair price of an option arises from the assumptions made under a given financial market model. The increasing complexity of these market assumptions contributes to the popularity of the numerical treatment of option valuation. Therefore, the pricing and hedging of plain vanilla options under the Black–Scholes model usually serve as a benchmark for the development of new numerical pricing approaches and methods designed for advanced option pricing models. The objective of the paper is to present and compare the methodological concepts for the valuation of simple vanilla options using the relatively modern numerical techniques in this issue which arise from the discontinuous Galerkin method, the wavelet approach and the fuzzy transform technique. A theoretical comparison is accompanied by an empirical study based on the numerical verification of simple vanilla option prices. The resulting numerical schemes represent a particularly effective option pricing tool that enables some features of options that are dependent on the discretization of the computational domain as well as the order of the polynomial approximation to be captured better.

Keywords

Black–Scholes equation, discontinuous Galerkin method, fuzzy transform, option pricing, wavelet method.

JEL Classification: B23, C44, G13

* jiri.hozman@tul.cz (corresponding author)

The authors were supported through the *Czech Science Foundation (GACR) under project 16-09541S and SP2018/34*, an SGS research project of VSB-TU Ostrava. The support is gratefully acknowledged.

Review of modern numerical methods for a simple vanilla option pricing problem

Jiří HOZMAN, Dana ČERNÁ, Michal HOLČAPEK, Tomáš TICHÝ, Radek VALÁŠEK

1. Introduction

During the last decades, both the options themselves and the financial models needed for their valuation have acquired increasing popularity. The simplest options, in other words vanilla options, as well as a number of more complex options, are currently the most frequently used financial instruments, whether the purpose of their holding is adjusting the investment profile, hedging or speculation. Therefore, valuing different types of option contracts plays a very important role in modern financial theory and practice. The determination of the fair price of an option is thus an essential task that is typically formulated by various partial differential equations (PDEs), for which analytical solutions can be derived in a closed form only under very restrictive conditions.

With increasing complexity, closed-form formulae are no longer readily available, so a wide range of studies have focused on the numerical realization of the option pricing problem, ranging from stochastic simulations (see Glasserman, 2003) to numerical solutions of PDEs using finite difference methods (FDMs) (e.g., Duffy, 2006) or variational techniques (e.g., Topper, 2005).

In this paper, we focus on three relatively novel numerical techniques in the field of financial engineering, based on the discontinuous Galerkin method (DGM), the wavelet methods (WM) and the fuzzy transform technique (FT), which all fall into the class of variation methods. These new approaches represent a very powerful tool for the numerical simulation of option pricing, because they allow us to capture better some features of different options under various market conditions with respect to the discretization of the computational domain as well as the order of the polynomial approximation.

The DGM combines the ideas and techniques of the finite volume method (FVM) and the finite element method (FEM) to take advantage of their strengths while eliminating their shortcomings. The FEM is a high-order method that is primarily designed for problems for which the exact solution is sufficiently regular and no steep derivatives or discontinuities in the data or solutions are presented. The starting point is a variational formulation of the solved PDE and a concept of a weak solution as an element of the suitable infinite-

dimensional function space (usually called the space of test functions). Then, we can compute a discrete solution using the Ritz–Galerkin method as soon as a finite-dimensional subspace of the space of test functions is specified. There are various ways to define these spaces. However, they are typically constructed as spaces of continuous piecewise polynomial functions with respect to the decomposition of the computational domain into finite elements. The basis of such a space is finite and is formed by the basis functions that generate the whole space. Therefore, the FEM in its simplest form can be observed as a special way of constructing these spaces, which are called finite element spaces; see Ciarlet (1978).

On the other hand, the FVM based on discontinuous, piecewise constant approximations allows us to capture discontinuities in the solution but has a low order of accuracy. The FVM was originally developed for the discretization of conservation laws. Similarly to the FDM, the values are calculated at discrete places in a meshed geometry. The essential idea is to divide the domain into many discretization cells, called finite volumes, and approximate the integral conservation law for each of these volumes. More precisely, the volume integrals in the solved PDE that contain a divergence term are converted into surface ones using the divergence theorem. Then, these terms are evaluated using the numerical fluxes that are conserved from one finite volume to its neighbour; that is, the flux entering a given volume is identical to that leaving the adjacent one. This feature is called local conservativity. To construct the discrete solution, we assume that the solution in each finite volume is constant; thus, the finite volume approach produces the piecewise constant approximations related to the discrete unknowns (see Eymard et al., 2000). Taking all of the above into account, the DGM can be viewed as a generalization of the finite-volume techniques into higher-order schemes or as an imaginary bridge between the finite element and the finite volume.

The DGM provides the numerical solution of the PDEs composed of piecewise polynomial functions on a finite-element mesh without any requirements for the continuity of the solution across particular elements. Therefore, this approach is suitable for problems for which other techniques fail or have difficulties. Although the DGM was developed in the early 1970s (see

Reed and Hill, 1973), its potency in option pricing problems has not been fully exploited yet. From this point of view, this method represents a very promising numerical tool.

Wavelet methods use wavelets as basis functions. Wavelets are known for their compression property, which means that they allow sparse representation of a wide range of functions and operators. Their advantage is that they form a Riesz basis for Sobolev spaces, which ensures the stability of the computation and the small condition number of the matrices arising from the discretization of partial differential equations. Wavelets can be constructed as piecewise polynomial functions of any order and thus allow the approximation of a high order for a wide class of functions. These interesting wavelet properties have led to the design of effective adaptive methods for solving differential, integral and integro-differential equations. Let us mention, for example, the general concept for solving operator equations using wavelets, which was designed by Cohen et al. (2002) and modified in many other works. The advantage of methods based on these ideas is the small number of parameters representing the solution with desired accuracy. The aforementioned high-order approximation of functions leads to high-order adaptive methods. The small condition number of the diagonally preconditioned discretization matrices results in a relatively small number of iterations needed to determine the solution with the required accuracy. It has been demonstrated that, for a wide class of problems, these methods are asymptotically optimal; that is, the computation time depends linearly on the number of parameters representing the solution. Another advantage is that the matrices arising from discretization can be represented by sparse matrices in the case of partial differential equations and partial integro-differential equations, for example equations representing jump diffusion models for option pricing, whereas classical methods lead to full matrices. Wavelet methods have already been used for option pricing (see, e.g., Hilber et al., 2005, 2013; Li et al., 2014). In this paper, we present a method that is based on some of the ideas of Cohen et al. (2002) but that is more efficient in our numerical experiments.

The third numerical method considered in this article is based on the fuzzy transform (F-transform for short) technique. The F-transform technique was introduced by Perfilieva (2003) to approximate real valued functions usually from L^2 space and has two phases: direct and inverse. The direct F-transform transforms a continuous (or integrable) function defined in a bounded interval into a finite vector of real numbers, which are called the components of the F-transform. The inverse F-transform returns the vector of the F-transform components to a continuous function that approximates the original function. The key parameter of

the F-transform is a fuzzy partition of the domain of the considered functions by means of fuzzy sets that form the basis function. Setting fuzzy partitions affects the quality of the approximation of functions using the F-transform. The first application of the F-transform in the numerical solution of ordinary differential equations, in particular the Cauchy problem, was described by Perfilieva (2003) and partial differential equations of special types for multivariable functions by Štěpnička and Valášek (2003, 2005). A generalization of the previous method of the numerical solution of partial differential equations was then proposed by Holčapek and Valášek (2017). The principal of the numerical solution of ordinary or partial differential equations consists of the substitution of the respective F-transform components for all the functions and their (partial) derivatives in the differential equation. The F-transform components of the derivatives of functions are then expressed by the method of finite differences (cf. Duffy, 2006). The result of the substitution of the F-transform components and the expression of derivatives is a system of linear algebraic equations with unknown F-transform components of a function, which is a solution of the differential equation. The approximate solution of the differential equation is obtained by the inverse F-transform. The contribution of the F-transform to the numerical solution of differential equations consists mainly of the reduction of the number of linear algebraic equations, the solution of which becomes very complex for an increasing dimension of function spaces.

The aim of the paper is to formulate the option pricing problem using the three above-mentioned methods to develop methodological concepts for a comparison on preliminary numerical experiments. The paper is organized as follows. After specifying the option pricing problem in the forthcoming section, attention is paid to the particular methods (Sections 3 to 5). Next, in Section 6, a simple numerical comparison is performed. Within the concluding remarks, in Section 7, we discuss the common features of the methods presented and the differences between them.

2. Option pricing problem

In this paper, we focus only on the simplest case of options, such as European vanilla options – this type of options can be exercised only at maturity T and the payout is determined on the basis of the difference in the value or price of the underlying asset x and the strike price K . If this difference is positive, we say that an option contract is in the money (ITM), in the case of a negative difference, it is out of the money (OTM), and, finally, for equality of prices, we talk about at the money options (ATM), the prices of which are the most sensitive to a change in the input parameters.

The problem of determining the (fair) price of option $u = u(x, t)$ (at time to maturity t and depending on the value of the underlying factor x , e.g., the price of the underlying stock or stock index) can be formulated as the following non-stationary partial differential equation:

$$\frac{\partial u}{\partial t} + \mathcal{L}_{BS}(u) = 0 \text{ in } \mathbb{R}^+ \times (0; T) \quad (1)$$

with the linear operator

$$\mathcal{L}_{BS}(u) = -\frac{1}{2}\sigma^2 x^2 \frac{\partial^2 u}{\partial x^2} - rx \frac{\partial u}{\partial x} + ru, \quad (2)$$

where the constants r and σ are the risk-free interest rate and the volatility of the underlying factor, respectively.

Formulation (1)–(2) is known in the literature as the Black–Scholes (BS) equation and describes the development of the price of the vanilla option; see the pioneering papers by Black and Scholes (1973) and Merton (1973). From the mathematical point of view, this equation represents a convection–diffusion problem that has to be equipped with a suitable set of initial and boundary conditions to be well posed.

For simplicity, we restrict our investigation to the case of the put option. Supposing the reversal time running, the initial condition is determined as a piecewise linear function (i.e., payoff) based on strike price K as follows:

$$u(x, 0) = \max(K - x, 0), \quad x \in \mathbb{R}^+. \quad (3)$$

Thus, it is obvious that, for example, ITM options will be obtained at $K > x$, whereas $x < K$ leads to the OTM options (for the call options hold the opposite).

Further, we prescribe the boundary conditions of the Dirichlet type at both endpoints of the computational domain $\Omega = (0; S_{max})$, i.e.,

$$u(0, t) = Ke^{-rt}, \quad t \in (0; T), \quad (4)$$

$$u(S_{max}, t) \approx 0, \quad t \in (0; T). \quad (5)$$

Condition (4) comes from the so-called put–call parity, and relation (5) is based on the asymptotic behaviour of the exact solution of the problem, in which the option price in a sufficiently large finite value S_{max} is approximated by asymptotic values at infinity. Other possible choices of boundary conditions are given by Hozman and Tichý (2016).

Since boundary conditions are not homogeneous, we introduce the function

$$z(x, t) = Ke^{-rt} \left(1 - \frac{x}{S_{max}}\right), \quad (6)$$

to transform them into homogeneous ones. If we assume $u^* = u - z$, then, after simple manipulation, we obtain a new equation:

$$\frac{\partial u^*}{\partial t} + \mathcal{L}_{BS}(u^*) = g \text{ in } \Omega \times (0; T) \quad (7)$$

with homogeneous boundary conditions and the initial condition

$$u^*(0, t) = u^*(S_{max}, t) = 0, \quad t \in (0; T), \quad (8)$$

$$u^*(x, 0) = \max(K - x, 0) - K \left(1 - \frac{x}{S_{max}}\right), \quad x \in \Omega, \quad (9)$$

where

$$g(x, t) = -e^{-rt} \frac{Krx}{S_{max}}. \quad (10)$$

If u^* is the solution of (7), then the solution of (1) restricted to Ω is the function $u = u^* + z$. The analytical solution of (1) at time t is

$$u(x, t) = -x \Phi(-d) + Ke^{-rt} \Phi(-d + \sigma\sqrt{t}),$$

$$d = \frac{\ln\left(\frac{x}{K}\right) + \left(r + \frac{\sigma^2}{2}\right)t}{\sigma\sqrt{t}}, \quad (11)$$

where Φ denotes the cumulative distribution function of the standard normal distribution. Finally, note that the relations mentioned above can be generalized simply in the case of call options and even extended relatively simply to a variety of exotic options; see, for example, Haug (1997).

3. Discontinuous Galerkin method

The discrete solution U_l^{DG} constructed by the DG method approximates the exact solution $u^*(x, t)$ in the time layer $t_l = l\tau$ (with a constant time step $\tau \equiv T/M$) for the whole computational domain Ω , that is,

$$U_l^{DG} \in S_h \equiv \{v \in L^2(\Omega); v|_{I_k} \in P_p(I_k) \forall I_k \in \mathcal{T}_h\}, \quad (12)$$

where \mathcal{T}_h is a partition of domain Ω and $P_p(I_k)$ denotes the space of all polynomials of order less than or equal to p defined for subintervals I_k of length h . For a complete overview of the DG technique, we refer the readers to the book by Rivière (2008). Further, the approximate values of U_l^{DG} at each time level $l\tau$ are calculated according to the following scheme:

$$\begin{aligned} & (U_{l+1}^{DG}, v) + \frac{\tau}{2} \mathcal{B}_h^{DG}(U_{l+1}^{DG}, v) \\ &= (U_l^{DG}, v) - \frac{\tau}{2} \mathcal{B}_h^{DG}(U_l^{DG}, v) \\ &+ \frac{\tau}{2} (g((l+1)\tau), v) \\ &+ \frac{\tau}{2} (g(l\tau), v) \quad \forall v \in S_h, \end{aligned}$$

$$l = 0, \dots, M-1, \quad (13)$$

wherein the initial state U_0^{DG} is defined as the S_h approximation of initial condition (9). The symbol (\cdot, \cdot) denotes the scalar product in the space $L^2(\Omega)$, the function g is defined in (10) and the bilinear form \mathcal{B}_h^{DG} includes the semi-discrete variants of diffusion, convection, penalty and reaction terms; for more details, see Hozman (2012).

Numerical scheme (13) can in fact be interpreted as a system of linear algebraic equations with a sparse matrix of the number of unknowns corresponding to the dimension of discrete space S_h , and the approximate solution U_l^{DG} can be expressed as a linear combination of basis functions, specifically

$$U_l^{DG} = \sum_{j=1}^{\text{DOF}} u_j^l \varphi_j, \quad (14)$$

where DOF (degrees of freedom) denotes the number of basis functions of space S_h . For ease of illustration, Figure 1 shows examples of linear basis functions and Figure 2 non-linear (quadratic) ones, all constructed on the uniform partition \mathcal{T}_h .

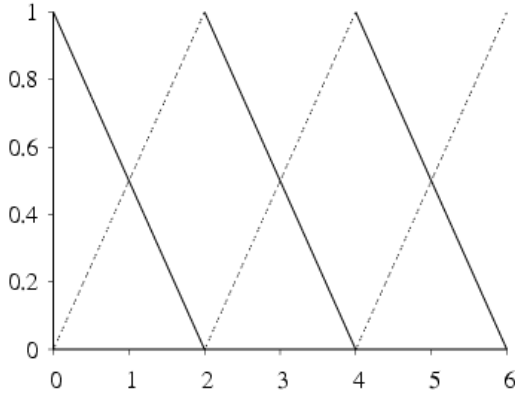


Figure 1 Linear basis functions: the horizontal axis represents a unit partition of fictitious computational domain and the vertical one the values of basis functions.

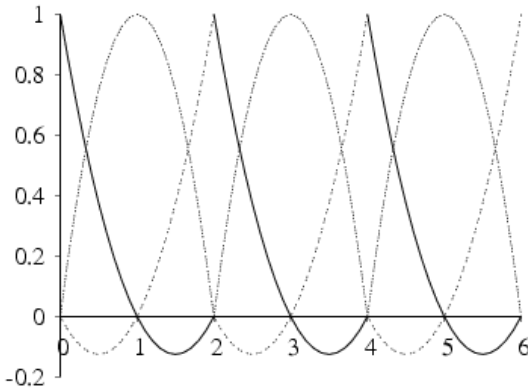


Figure 2 Quadratic basis functions: the horizontal axis represents a unit partition of fictitious computational domain and the vertical one the values of basis functions.

For each time layer t , we thus solve the problem

$$\left(\mathbb{M} + \frac{\tau}{2} \mathbb{B}\right) \mathbb{w}_{DG}^{l+1} = \left(\mathbb{M} - \frac{\tau}{2} \mathbb{B}\right) \mathbb{w}_{DG}^l + \frac{\tau}{2} \mathbb{g}^{l+1} + \frac{\tau}{2} \mathbb{g}^l \quad (15)$$

for the unknown vector of the basis coefficients $\mathbb{w}_{DG}^l = \{u_j^l\}$. Matrix $\mathbb{M} = (m_{ij})$, where $m_{ij} = (\varphi_j, \varphi_i)$ represents the mass matrix, and matrix $\mathbb{B} = (b_{ij})$, where $b_{ij} = \mathcal{B}_h^{DG}(\varphi_j, \varphi_i)$ and vector \mathbb{g}^l has components given by $(g(\tau t), \varphi_i)$. System (15) is then solved by a suitable linear algebraic solver, for example the generalized minimal residual method (GMRES), and the resulting approximate solution of (1)–(2) obtained by the DG method is of the form $U_M^{DG} + Z_M$, where Z_M is the S_h approximation of function z at time T .

4. Wavelet methods

First, we briefly introduce the concept of a wavelet basis. We focus on a one-dimensional wavelet basis defined in the interval $\Omega = (0; S_{max})$ for the space

$$V = \{v \in L^2(\Omega); v(0) = v(S_{max}) = 0\} \quad (16)$$

and Sobolev space $H_0^1(\Omega)$. We assume that H is one of these spaces and that J is an index set such that each index $\lambda \in J$ has the form $\lambda = (j, k)$, where $|\lambda| = j$ denotes the level. Set $\Psi = \{\psi_\lambda, \lambda \in J\}$ is called a wavelet basis for space H , if the following conditions are satisfied:

- *Riesz basis.* Ψ is a Riesz basis of H .
- *Locality.* For all $\lambda \in J$, the length of the support of ψ_λ is bounded by $C \cdot 2^{-|\lambda|}$, where C is a constant independent of $|\lambda|$.
- *Hierarchical structure.* Set Ψ has the structure

$$\Psi = \Phi_{j_0} \cup \bigcup_{j=j_0}^{\infty} \Psi_j. \quad (17)$$

The functions from $\Phi_j = \{\varphi_{j,k}, k \in I_j\}$ are called scaling functions, and the functions from $\Psi_j = \{\psi_{j,k}, k \in J_j\}$ are called wavelets on level j .

- *Vanishing wavelet moments.* We assume that $L \geq 1$ exists such that $\psi_{j,l}$ have L vanishing moments; that is, any polynomial p of degree $m \leq L-1$ satisfies

$$\int_{\Omega_{j,l}} p(x) \psi_{j,l}(x) dx = 0, \quad (18)$$

where $l \in J_j, j \geq j_0, \Omega_{j,l} = \text{supp } \psi_{j,l}$.

The definition of the wavelet basis is not unified in the literature, and some of the above conditions may be generalized in some cases.

In our numerical experiments, we use the linear and quadratic spline wavelet bases from Černá and Finěk (2011). Graphs of the selected linear and quadratic spline wavelets are shown in Figure 3 and Figure 4, respectively. In the case of a linear spline basis, a boundary wavelet $\psi_{2,1}$ and an inner wavelet $\psi_{2,2}$ are displayed. In the case of a quadratic basis, two boundary wavelets $\psi_{3,1}$ and $\psi_{3,2}$ and an inner wavelet $\psi_{3,3}$ are shown.

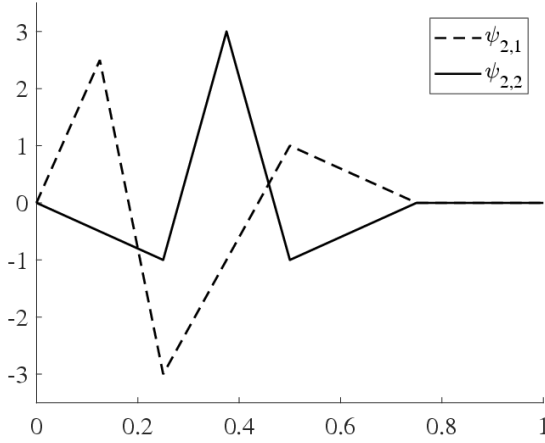


Figure 3 Linear spline wavelet basis functions: the horizontal axis represents a reference unit interval and the vertical one the values of basis functions.

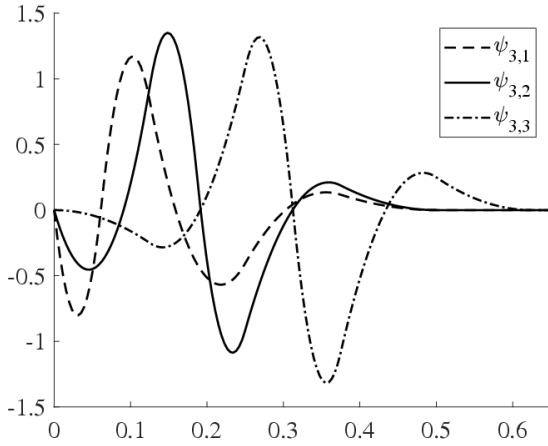


Figure 4 Quadratic spline wavelet basis functions: the horizontal axis represents a reference unit interval and the vertical one the values of basis functions.

We use the Crank–Nicolson scheme to discretize equation (7) in time. The introduced notation is analogous to that in the previous chapter; specifically, τ denotes the time step size and t_l denotes the corresponding time level. Furthermore, we denote $U_l(x) = u^*(x, t_l)$, $g_l(x) = g(x, t_l)$ and $\mathcal{B}^W(u, v) = (\mathcal{L}_{BS}(u), v)$ for $u, v \in H_0^1(\Omega)$. Then, the variational formulation of (7) has the form

$$\frac{(U_{l+1}, v)}{\tau} - \frac{\mathcal{B}^W(U_{l+1}, v)}{2} = \frac{\mathcal{B}^W(U_l, v)}{2} + \frac{(g_{l+1} + g_l, v)}{2} + \frac{(U_l, v)}{\tau} \quad (19)$$

for all $v \in H_0^1(\Omega)$. To increase the efficiency of the Crank–Nicolson scheme, Richardson's extrapolation can be used; see Finěk (2017).

For discretization with respect to the spatial variable x , we use the wavelet method. The adaptive wavelet method differs from classical approaches, because it is based not on local error estimates but on thresholding wavelet coefficients. Let $\Psi = \{\psi_\lambda, \lambda \in J\}$ be a wavelet basis of space V such that Ψ , when normalized with respect to the H^1 norm, is a wavelet basis of space $H_0^1(\Omega)$. We expand solution U_l in a wavelet basis Ψ , that is,

$$U_l = \sum_{\lambda \in J} u_\lambda^l \psi_\lambda. \quad (20)$$

We substitute (20) into (19) and obtain the bi-infinite system

$$\mathbb{A} \mathbb{w}^{l+1} = \mathbb{f}^l \quad (21)$$

where

$$\mathbb{w}^l = \{u_\lambda^l\}_{\lambda \in J}, \mathbb{A} = \{A_{\mu, \lambda}\}_{\mu, \lambda \in J}, \mathbb{f}^l = \{f_\mu^l\}_{\mu \in J} \quad (22)$$

and

$$A_{\mu, \lambda} = \frac{(\psi_\lambda, \psi_\mu)}{\tau} - \frac{\mathcal{B}^W(\psi_\lambda, \psi_\mu)}{2}, \lambda, \mu \in J, \quad (23)$$

$$f_\mu^l = \frac{(g_{l+1} + g_l, \psi_\mu)}{2} + \frac{\mathcal{B}^W(U_l, \psi_\mu)}{2} + \frac{(U_l, \psi_\mu)}{\tau}, \mu \in J. \quad (24)$$

We solve the resulting system using the method of generalized residuals (GMRES) with diagonal preconditioning. The algorithm comprises the following steps:

1. Choose the time step τ and the number of basis functions' DOFs.
2. Compute the vector of coefficients \mathbb{w}^0 for the function U_0 and $\mathbb{w}_W^0 = \text{COARSE}(\mathbb{w}^0, \text{DOF})$.
3. For $l = 0, 1, 2, \dots, M-1$, compute the right-hand side \mathbb{f}^l and calculate $\mathbb{w}^{l+1} = \text{GMRES}(\mathbb{A}, \mathbb{f}^l, \mathbb{w}_W^l)$ and $\mathbb{w}_W^{l+1} = \text{COARSE}(\mathbb{w}^{l+1}, \text{DOF})$.
4. Using \mathbb{w}_W^M , compute the approximate solution U_M^W of equation (7). The approximate solution of (1)–(2) is computed as $U_M^W + z_M$, where $z_M(x) = z(x, T)$.

In this algorithm, $\mathbb{w}^{l+1} = \text{GMRES}(\mathbb{A}, \mathbb{f}^l, \mathbb{w}_W^l)$ means that \mathbb{w}^{l+1} is the solution of the system with (bi-infinite) matrix \mathbb{A} and the right-hand side \mathbb{f}^l using the GMRES with initial vector \mathbb{w}_W^l . The routine $\mathbb{w}_W^{l+1} = \text{COARSE}(\mathbb{w}^{l+1}, \text{DOF})$ consists of thresholding, that is, taking DOF elements of vector \mathbb{w}^{l+1} , which are the highest in absolute value, and we set the others to zero. Then, output vector \mathbb{w}_W^{l+1} contains DOF non-zero ele-

ments. Each iteration of the GMRES requires the multiplication of infinite-dimensional matrix \mathbb{A} with the finite-dimensional vector. We compute this operation approximately following the method of Černá and Finěk (2013). Since we work with a sparse representation of the right-hand side and a sparse representation of the vector representing the solution, the method is adaptive. In our case, the most significant coefficients belong to wavelets with support close to strike K , because the initial function has a discontinuous derivative there and the coefficients in the areas where the function is smooth are very small and can be thresholded.

5. F-transform

The F-transform was proposed by Perfilieva (2003) as a new approximate technique based on the tools of fuzzy modelling to transform functions of $L^2(\Gamma)$ space, where $\Gamma \subseteq \mathbb{R}^d$ is a compact convex subspace, into a finite system of real numbers, which provides compressed information about the original functions, and these numbers are then used for an approximate continuous reconstruction of the original functions from $L^2(\Gamma)$ space. The core of the F-transform consists of a fuzzy partition of domain Γ using a system of fuzzy sets $\Phi = \{\varphi_k(x) ; k \in \mathbb{K}, x \in \Gamma\}$, where $\mathbb{K} \subseteq \mathbb{N}^d$ is a finite index set, for which the following Ruspini condition holds:

$$\sum_{k \in \mathbb{K}} \varphi_k(x) = 1, x \in \Gamma. \quad (25)$$

Fuzzy set φ_k refers to the k -th basis function of fuzzy partition Φ . Below, we briefly describe the F-transform technique and its application to the numerical solution of the partial differential equation. As we mentioned in Section 1, we distinguish two phases of the F-transform, namely direct and inverse. The direct F-transform with respect to fuzzy partition Φ transforms each function u from $L^2(\Gamma)$ space into a finite system of real numbers $\mathcal{F} = \{F_k; k \in \mathbb{K}\}$, where

$$F_k = \int_{\Gamma} u(x) \varphi_k(x) dx / \int_{\Gamma} \varphi_k(x) dx, k \in \mathbb{K}. \quad (26)$$

The real number F_k determined by formula (26) is called the k -th F-transform component, which is the weighted average of u at node x_k with respect to the basis functions φ_k of fuzzy partition Φ . The inverse F-transform of function u with respect to fuzzy partition Φ provides a continuous function $\mathcal{F}[u]: \Gamma \rightarrow \mathbb{R}$, which is a linear combination of basis φ_k and F-transform components F_k , that is,

$$\mathcal{F}[u](x) = \sum_{k \in \mathbb{K}} F_k \varphi_k(x), x \in \Gamma. \quad (27)$$

Concerning the numerical solution of equation (1) with the help of the F-transform, we assume $\Gamma = [0; S_{max}] \times [0; T]$ and $\mathbb{K} = \{0, \dots, \text{DOF}\} \times \{0, \dots, M\}$, where $\text{DOF}, M > 1$. Note that Γ is a topological closure of the product of $\Omega \times (0; T)$. Further, we assume $h =$

S_{max}/DOF and $\tau = T/M$ and define the basis function $\varphi_{j,l}(x, t)$ for any $(j, l) \in \mathbb{K}$ as

$$\varphi_{j,l}(x, t) = \mathcal{K}\left(\frac{x-x_j}{h}\right) \mathcal{K}\left(\frac{t-t_l}{\tau}\right), (x, t) \in \Gamma, \quad (28)$$

where $x_j = jh, t_l = l\tau$ and $\mathcal{K}: \mathbb{R} \rightarrow [0; \infty)$ is a continuous function that is even and non-decreasing in the interval $[-1; 0]$, $\mathcal{K}(0) = 1, \mathcal{K}(-1) = 0$, and it holds that $\int_{-\infty}^{+\infty} \mathcal{K}(t) dt = 1$. Function \mathcal{K} is called the generating function. Two examples of generating functions that are often used in practice can be seen in Figures 5 and 6.

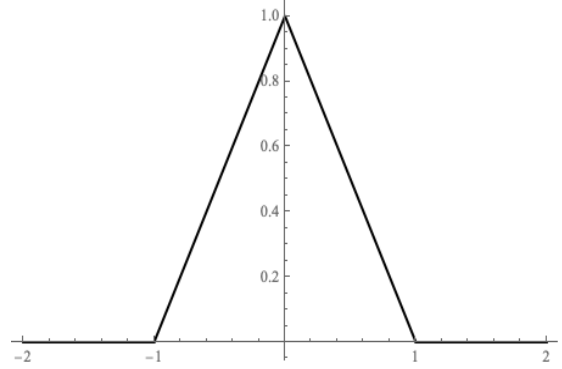


Figure 5 Triangular generating function: the horizontal axis represents a unit partition of fictitious computational domain and the vertical one the values of this basis function.

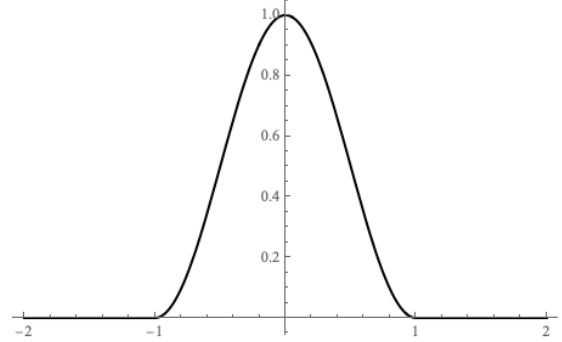


Figure 6 Raised cosine generating function: the horizontal axis represents a unit partition of fictitious computational domain and the vertical one the values of this basis function.

Differential equation (1) is solved similarly to that in the case of the method of finite differences, the only difference being that the function values at nodes x_j are replaced by their F-transform components. To apply the F-transform, differential equation (1) is transformed into homogeneous equation (7). Using the Crank–Nicolson method for time discretization, we transform differential equation (7) into the following equation:

$$\frac{u^*(x, t_{l+1}) - u^*(x, t_l)}{\tau} = -\frac{1}{2} \left(\mathcal{L}_{BS}(u^*(x, t_{l+1})) + \mathcal{L}_{BS}(u^*(x, t_l)) - g(x, t_{l+1}) - g(x, t_l) \right). \quad (29)$$

Further, we substitute the partial derivatives of function u^* with their F-transform components U_k^{FT} , which

are then expressed by the finite differences between components U_k^{FT} . As a result, we obtain the following equation:

$$\frac{U_{j,l+1}^{FT} - U_{j,l}^{FT}}{\tau} = -\frac{1}{2}(\mathcal{L}_{BS}(U_{j,l+1}^{FT}) + \mathcal{L}_{BS}(U_{j,l}^{FT}) - G_{j,l+1} - G_{j,l}), \quad (30)$$

where $G_{j,l+1}$ and $G_{j,l}$ are the F-transform components of function g and

$$\mathcal{L}_{BS}(U_{j,*}^{FT}) = -\frac{1}{2}\sigma^2 x_j^2 \frac{U_{j+1,*}^{FT} - 2U_{j,*}^{FT} + U_{j-1,*}^{FT}}{h^2} - r x_j \frac{U_{j+1,*}^{FT} - U_{j,*}^{FT}}{h} + r U_{j,*}^{FT}. \quad (31)$$

Let $\mathbb{U}_{FT}^l = \{U_{j,l}^{FT}\}$ denote the vector of the F-transform components of function u^* . Then, by simple manipulation, one can find the following system of linear algebraic equations:

$$\mathbb{A}\mathbb{U}_{FT}^{l+1} = \mathbb{B}\mathbb{U}_{FT}^l + \mathbb{d}^l, \quad l = 0, \dots, M-1 \quad (32)$$

with two three-diagonal matrices

$$\mathbb{A} = \begin{pmatrix} b_1 & c_1 & 0 & \dots & 0 \\ a_2 & b_2 & c_2 & \ddots & \vdots \\ 0 & \ddots & \ddots & \ddots & 0 \\ \vdots & \ddots & a_{\text{DOF}-2} & b_{\text{DOF}-2} & c_{\text{DOF}-2} \\ 0 & \dots & 0 & a_{\text{DOF}-1} & b_{\text{DOF}-1} \end{pmatrix}, \quad (33)$$

$$\mathbb{B} = \begin{pmatrix} b_1 & -c_1 & 0 & \dots & 0 \\ -a_2 & b_2 & -c_2 & \ddots & \vdots \\ 0 & \ddots & \ddots & \ddots & 0 \\ \vdots & \ddots & -a_{\text{DOF}-2} & b_{\text{DOF}-2} & -c_{\text{DOF}-2} \\ 0 & \dots & 0 & -a_{\text{DOF}-1} & b_{\text{DOF}-1} \end{pmatrix}, \quad (34)$$

where it holds for any $j = 1, \dots, \text{DOF} - 1$ that

$$a_j = \frac{1}{4}\sigma^2 x_j^2 \frac{\tau}{h^2}, \quad b_j = 1 - \left(\frac{\sigma^2 x_j^2}{h^2} + \frac{r x_j}{h} + r \right) \frac{\tau}{2}, \quad (35)$$

$$c_j = \left(\frac{\sigma^2 x_j^2}{2h^2} + \frac{r x_j}{h} \right) \frac{\tau}{2}$$

and $\mathbb{d}^l = \{(G_{j,l+1} + G_{j,l})\frac{\tau}{2}\}$ is the vector determined from the F-transform components of function g .

Using the initial homogeneous boundary conditions, namely $U_{j,0}^{FT} = u(x_j, 0)$ for $j = 0, \dots, \text{DOF}$ and $U_{0,l}^{FT} = U_{\text{DOF},l}^{FT} = 0$ for $l = 0, \dots, M$, one can simply solve the previous system of linear algebraic equations, and the solution can be expressed by the F-transform matrix:

$$\mathcal{F} = \begin{pmatrix} 0 & 0 & \dots & 0 \\ u(x_1, 0) & U_{1,1}^{FT} & \dots & U_{1,M}^{FT} \\ \vdots & \vdots & \ddots & \vdots \\ u(x_{\text{DOF}-1}, 0) & U_{\text{DOF}-1,1}^{FT} & \dots & U_{\text{DOF}-1,M}^{FT} \\ 0 & 0 & \dots & 0 \end{pmatrix}. \quad (36)$$

The approximate solution of function u^* is obtained by the inverse F-transform as follows:

$$\mathcal{F}[u^*](x, t) = \sum_{(k,l) \in \mathbb{K}} U_{k,l}^{FT} \varphi_{k,l}(x, t), \quad (x, t) \in \Gamma. \quad (37)$$

The approximate solution of the differential equation (1) is determined by the transformation $u = u^* + z$ described above, where z is the function transforming equation (1) into the homogeneous form.

6. Numerical experiments

The numerical experiment presented below is based on data modified from Kopa et al. (2017) and especially Hozman and Tichý (2014), who provide a vanilla put option pricing case study of German option market (on September 15, 2011) using DG approach. We consider here one particular scenario only – intermediate maturity option (193 calendar days) on DAX (German stock market index) with current index value 4,715 and the strike price 4,700, indicating a near ATM option. The fixed BS parameters of the model are the risk-free interest rate $r = 0.039$ and the volatility $\sigma = 0.4422$. The relevant volatility value is set as the weighted average of observed implied volatilities, and the risk-free interest rate is determined based on this fixed volatility and the option price given by the analytical formula (11).

Numerical approximation is crucially related to the discretization of the computational domain Ω , its length is deliberately chosen as eight times the strike price to suppress the influence of the inaccurate homogenous Dirichlet boundary condition (5). Together with this, we choose the time step $\tau = \frac{1}{3600}$ so that the effect of time discretization on numerical results is negligible. For a more detailed comparison, each of the methods is considered in the form of linear as well as nonlinear (quadratic, cosine) approximation. The quality of the approximation can be easily observed by comparing the numerical results with the theoretical prices from (11). Therefore, we can consider relative error in the $L^2(\Omega)$ -norm on the whole computational domain evaluated at maturity, i.e.,

$$e_{L^2} = \frac{\sqrt{\int_{\Omega} (u_M - u(T))^2 dx}}{\sqrt{\int_{\Omega} u^2(T) dx}} \quad (38)$$

where u_M denotes the approximate solution obtained by one of the three numerical approaches.

The results of corresponding errors in a logarithmic scale are illustrated in Figure 7. In all cases we can observe a monotone decrease of the relative errors with increasing number of basis functions. More precisely, for linear approximations (denoted as P1), all methods

have the same order of accuracy, which is expected as quadratic. In contrast, the results for nonlinear basis functions (denoted as P2 and cos) have a totally different character amongst the methods. The best performance is achieved by WM that shows a third order of accuracy for a quadratic basis. In the case of DGM, relative errors are smaller than for linear basis functions, however, they show the same trend as in the linear case, according to which DGM with quadratic approximations can be considered as a method with a quadratic order of accuracy. On the other hand, the results obtained by FT approach, in the case of raised cosine basis functions, do not lead to any improvement compared to the linear case and are almost identical.

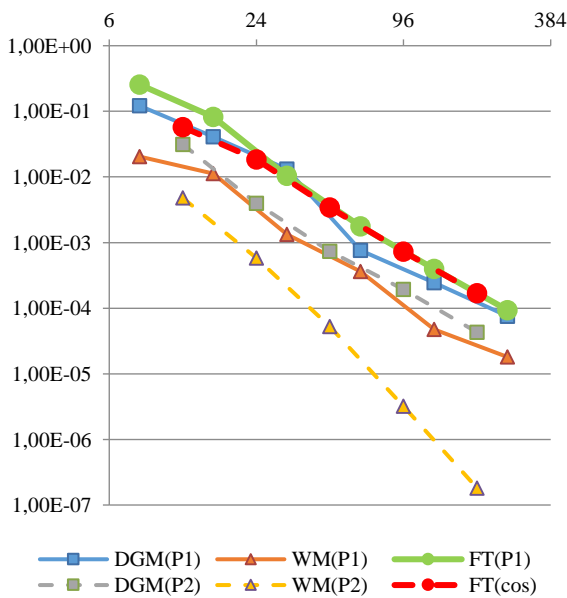


Figure 7 The comparison of relative errors of the numerical solution for particular methods with linear (solid line) and nonlinear (dashed line) approximations: the horizontal axis represents a number of degrees of freedom and the vertical one the values of relative errors.

Following the observations above, note that the results for DGM and WM correspond to the experimental properties of these methods, well-known for the class of convection-diffusion problems, see Rivière (2008) and Cohen et al. (2002), respectively. Since the FT approach is a relatively novel way, the results cannot be objectively compared, but serve as an important starting point for further development of this method.

7. Conclusion

In this paper, we briefly summarize the basic knowledge of option pricing and present three relatively novel approaches to the numerical solution of the BS equation governing vanilla option prices. The first nu-

merical scheme is derived from the discontinuous Galerkin method, which is based on discontinuous piecewise polynomial approximations. In contrast, wavelet methods employ continuous approximations and a basis with a hierarchical structure. The last technique is based on the F-transform, the application of which to the original continuous problem leads to a new one for the unknown components of this transform. The resulting problem is then discretized using the finite difference method.

The potential of each of the three methods is demonstrated within a simple experimental study. In the case of linear approximation, the results are very similar amongst all the methods, but, for non-linear basis functions, the differences in these approaches should be significant, especially due to the different types of basis functions (parabola vs. raised cosine). The wavelet approach has the best approximation properties for numerical solutions of the BS model. On the other hand, the benefits of F-transform could mainly be reflected in the possibility of reducing the number of degrees of freedom in the discretization under the preserved order of accuracy, which actually leads to the shortening of the computational time. However, this advantage of the F-transform will be observable mainly in solving the BS equation containing several underlying factors, in which the complexity of the calculation grows exponentially. Regarding the discontinuous Galerkin method, its main advantages are discontinuous pay-off functions and discrete sampling.

Apart from the detailed experimental study, emphasis will be placed further on extending these numerical schemes to the valuation of options with more complex pay-off functions (i.e., exotic options) and more detailed analysis of the sensitivity measures (simply called the Greeks). At the same time, the stochastic models for the standard parameters of option pricing models should be considered instead of the existing deterministic description, so the results obtained are closer to the market reality and correspond to the conclusions presented in this paper. This should provide more comprehensive information on the relationships amongst the presented methods.

References

- BLACK, F., SCHOLES, M. (1973). The pricing of options and corporate liabilities. *Journal of Political Economy* 81: 637–659. <https://doi.org/10.1086/260062>
- CIARLET, P. G. (1978). *The Finite Elements Method for Elliptic Problems*. North-Holland, Amsterdam, New York: Oxford. [https://doi.org/10.1016/S0168-2024\(08\)70178-4](https://doi.org/10.1016/S0168-2024(08)70178-4)

- COHEN, A., DAHMEN, W., DEVORE, R. (2002). Adaptive Wavelet Methods II – Beyond the Elliptic Case. *Foundations of Computational Mathematics* 2: 203–245. <https://doi.org/10.1007/s102080010027>
- ČERNÁ, D., FINĚK, V. (2013). Approximate multiplication in adaptive wavelet methods. *Central European Journal of Mathematics* 11: 972–983. <https://doi.org/10.2478/s11533-013-0216-x>
- ČERNÁ, D., FINĚK, V. (2011). Construction of optimally conditioned cubic spline wavelets on the interval. *Advances in Computational Mathematics* 34: 219–252. <https://doi.org/10.1007/s10444-010-9152-5>
- DUFFY, D.J. (2006). *Finite Difference Methods in Financial Engineering: A Partial Differential Equation Approach*. Chichester: John Wiley & Sons. <https://doi.org/10.1002/9781118673447>
- EYMARD, R., GALLOUËT, T., HERBIN, R. (2000). Finite volume methods. In *Solution of Equation in \mathbb{R}^n (Part 3), Techniques of Scientific Computing (Part 3). Handbook of Numerical Analysis* 7: 713–1018. [https://doi.org/10.1016/S1570-8659\(00\)07005-8](https://doi.org/10.1016/S1570-8659(00)07005-8)
- FINĚK, V. (2017). Fourth order scheme for wavelet based solution of Black-Scholes Equation. *AIP Conference Proceedings* 1910, No. 030004. <https://doi.org/10.1063/1.5013963>
- GLASSERMAN, P. (2003). *Monte Carlo Methods in Financial Engineering*. New York: Springer. <https://doi.org/10.1007/978-0-387-21617-1>
- HAUG, E. G. (1997). *The Complete Guide to Option Pricing Formulas*. 2nd edition, New York: McGraw-Hill.
- HILBER, N., MATACHE, A.M, SCHWAB, C., (2005). Sparse wavelet methods for option pricing under stochastic volatility. *Journal of Computational Finance* 8: 1–42. <https://doi.org/10.21314/JCF.2005.131>
- HILBER, N., REICHMANN, O., SCHWAB, C., WINTER, C. (2013). *Computational Methods for Quantitative Finance*. Berlin: Springer. <https://doi.org/10.1007/978-3-642-35401-4>
- HOLČAPEK, M., VALÁŠEK, R. (2017). Numerical solution of partial differential equations with the help of fuzzy transform technique. In *Proc. of 2017 International Conference on Fuzzy Systems (FUZZ-IEEE)*: 1–6. <https://doi.org/10.1109/FUZZ-IEEE.2017.8015742>
- HOZMAN, J. (2012). Discontinuous Galerkin Method for the numerical solution of option pricing. *Aplimat – Journal of Applied Mathematics* 5: 197–206.
- HOZMAN, J., TICHÝ, T. (2016). On the impact of various formulations of the boundary condition within numerical option valuation by DG method. *Filomat* 30: 4253–4263. <https://doi.org/10.2298/FIL1615253H>
- HOZMAN, J, TICHÝ, T. (2014). Black-Scholes option pricing model: Comparison of h -convergence of DG method with respect to boundary condition treatment. *ECON – Journal of Economics, Management and Business* 24(4): 141–152.
- KOPA, M., VITALI, S., TICHÝ, T., HENDRYCH, R. (2017). Implied volatility and state price density estimation: Arbitrage analysis. *Computational Management Science* 14(4): 559–583. <https://doi.org/10.1007/s10287-017-0283-8>
- LI, H., DI, L., WARE, A., YUAN, G. (2014). The applications of partial integro-differential equations related to adaptive wavelet collocation methods for viscosity solutions to jump-diffusion models. *Applied Mathematics and Computation* 335: 246–316. <https://doi.org/10.1016/j.amc.2014.08.002>
- MERTON, R.C. (1973). Theory of rational option pricing. *The Bell Journal of Economics and Management Science* 4: 141–18. <https://doi.org/10.2307/3003143>
- PERFILIEVA, I. (2003). Fuzzy transform: Application to the reef growth problem. In *Fuzzy Logic in Geology, R. Demicco and G. Klir, Eds.* Amsterdam: Academic Press, chapter 9: 275–300. <https://doi.org/10.1016/B978-012415146-8/50012-3>
- REED, W.H., HILL, T.R. (1973). Triangular mesh methods for the neutron transport equation. *Technical Report LA-UR-73-479*, Los Alamos Scientific Laboratory.
- RIVIÈRE, B. (2008). *Discontinuous Galerkin Methods for Solving Elliptic and Parabolic Equations: Theory and Implementation*, Philadelphia: Society for Industrial and Applied Mathematics. <https://doi.org/10.1137/1.9780898717440>
- ŠTĚPNIČKA, M., VALÁŠEK, R. (2005). Numerical solution of partial differential equations with help of fuzzy transform. In *Proc. of the 14th IEEE International Conference on Fuzzy systems*, 1153–1162. <https://doi.org/10.1109/FUZZY.2005.1452549>.
- ŠTĚPNIČKA, M., VALÁŠEK, R. (2003). Fuzzy transforms and their application to wave equation. *Journal of Electrical Engineering* 55(12): 7–10.
- TOPPER, J. (2005). *Financial Engineering with Finite Elements*, Chichester: John Wiley & Sons.

